Sofia University "St. Kliment Ohridski"
Faculty of Physics
Department Meteorology and Geophysics

Terrestrial water storage anomaly during the 2007 heat wave in Bulgaria

Master Thesis

of

Biliana Rumenova Mircheva
f.n. 180073

Thesis supervisor:

/Assoc. prof. G. Guerova/

Head of Department:

/Assoc. prof. N. Rachev/

Reviewer:

/Head assist. prof. M. Tsekov/

Sofia April 2016

Contents

List of Figures

List of Tables

Abstract

Heat waves have large adverse social, economic and environmental effects including increased mortality, transport restrictions and a decreased agricultural production. The estimated economic losses of the 2007 heat wave in Southeast Europe exceed 2 billion EUR with 19 000 hospitalisation in Romania only. The aim of this study is to investigate the anomalies of temperature, precipitation, integrated water vapour (IWV) and terrestrial water storage (TWS) in 2007 compared to 2003-2013, that could have lead to the heat wave.

The heat wave month (July 2007) was 2° C hotter than the 2003-2013 mean in Sofia, Bulgaria. The 2007 annual precipitation was on 10 % higher than the 2003-2013 mean, but in spring the negative precipitation anomaly in April was followed by a large positive anomaly in May. A large negative precipitation anomaly is recorded in July 2007. In alignment with the precipitation, IWV computed from a GNSS station in Sofia shows a large positive anomaly in May 2007, while a negative anomaly in July. The terrestrial water storage anomaly, derived from the GRACE mission, has one month of delay and with a negative anomaly recorded in August 2007. It is possible that is due to the slower soil response to the atmospheric drying and the heat.

Intercomparison is performed for the period 2003-2008 with ALADIN-Climate regional climate model. The following can be concluded for 2007 anomalies in the model and observations: 1) a strong correlation for temperature and IWV anomalies data sets and 2) a weak relation between the precipitation and TWS anomalies data set.

Chapter 1

Introduction

Climate change include variations in water and energy cycles on Earth. According to *Stocker et al.* (2013) the global mean temperature increases year after year with 2015 being the hottest year in the records. Higher global temperature leads to changes in the hydrological cycle. For example increase of temperature with 1° C leads to 7 % increase in water vapour, in agreement with the Clausius-Clapeyron equation (*Dai*, 2006). Thus more water is evaporated providing appropriate conditions for intensive and powerful storms, reducing the ground water content and increasing in the frequency of occurrence of extreme weather events in different parts of the world (*Matzarakis et al.*, 2007).

Presented in figure 1.1 are the components of hydrology cycle: water vapour, liquid water, rain and water storage on earth surface and below. A complete description of the global water cycle is still a challenge. At present, the hydrology cycle components like evaporation, cloud formation, evapo-transpiration, soil moisture content are studied in isolation and integrated in some way using computer models (*Trenberth et al.*, 2006). Despite the efforts, the global picture of the hydrology cycle and its changes is still unclear. There is a lack of information due to the difficulties of collecting data over oceans and other inaccessible terrains. There are uncertainties in quantities of river run-off, stream flows, ice sheets and groundwater content. Routine monitoring of hydrology components requires the collection and processing of large quantity of data.

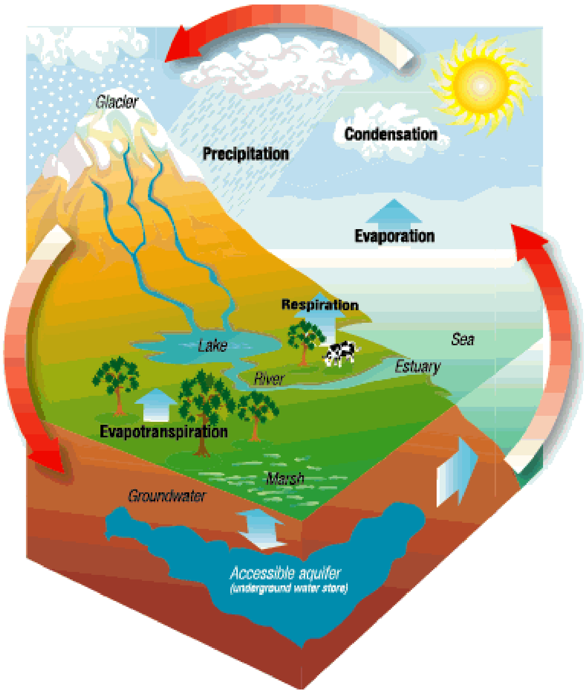

Figure 1.1: Water cycle components, image credit: web (b).

Essential component of the hydrology cycle is the Terrestrial Water Storage (TWS) defined as all forms of water above and beneath the surface of the Earth. TWS is an aggregation of the amounts of ground water, soil moisture, surface water, snow, ice and vegetation water content. Thus TWS variability is the sum of changes in snow, soil moisture, and ground water. TWS varies in space and time. For understanding TWS major role in the climate system it is necessary to measure and analyse its spatio-temporal variations by different methods. The TWS changes can be produced using combination of advanced land surface models for evaporation, precipitation and soil moisture content, reliable observations, and statistical assimilation techniques. Because of the complexity of TWS structure and components it is difficult to get a precise global or regional description. In the past decades satellite missions were the main source of data to study Earth's hydrological components including TWS.

One such missions is the Gravity Recovery And Climate Experiment (GRACE). GRACE is a polar orbiting twin satellite launched in 2002. GRACE

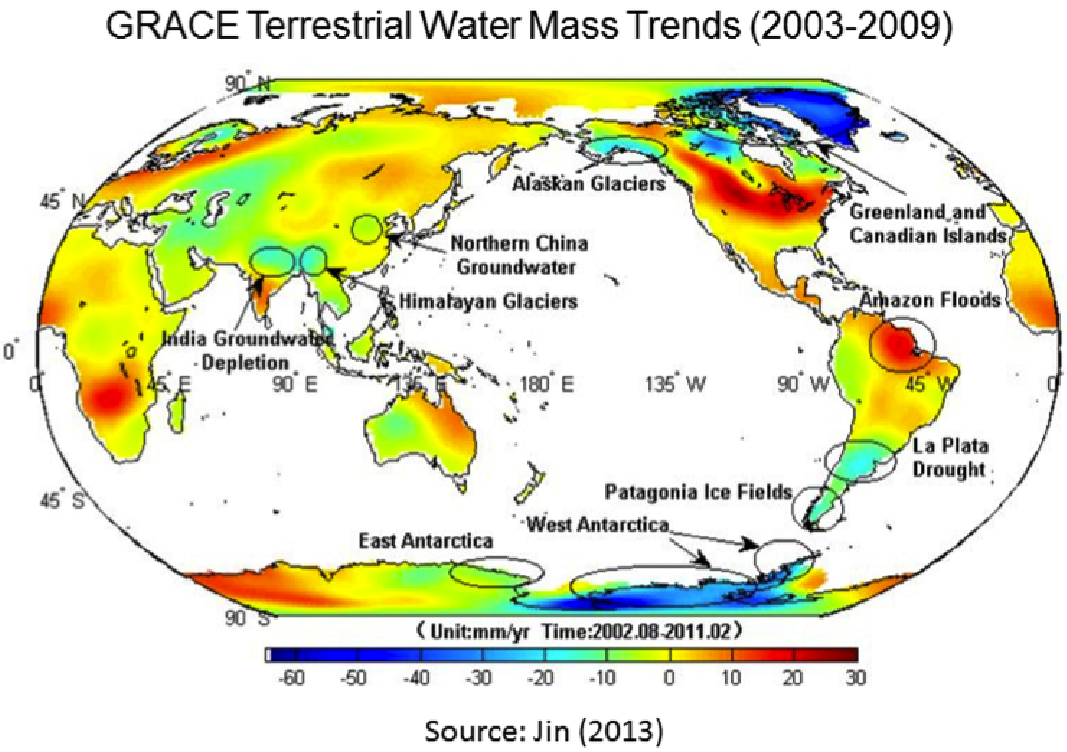

Figure 1.2: Global TWS anomaly trend for 2003-2009, image credit: web (c).

maps changes in Earth's gravity field, which can be converted to water mass variations and column-integrated TWS variations. The ability of obtaining information below the first several centimetres of the land surface is what makes GRACE so valuable for hydrological researches and applications such as drought monitoring. The GRACE mission has been completed, but the GRACE Follow-On (GRACE-FO) mission will be deployed in 2017 (web, e) and will be used to continue the monitoring of gravity anomalies. With its global coverage GRACE provides global maps of TWS anomalies. In figure 1.2 are shown the significant changes in terrestrial water mass trends, on a global scale that occurred between 2003 and 2009. For example there are losses in Alaskan and Himalayan glaciers, Greenland, Patagonia ice fields and West Antarctica. Also there is depletion of groundwater in India, Northern China, West Australia and La Plata in South America. According to GRACE data positive trends of TWS have areas in Amazon, East Australia and South Africa.

The anomaly of TWS has been studied worldwide. For example *Ramillien et al.* (2014) report that in South Africa, in the area of Zambezi river basin, there has been an increase of water mass since 2006. The results show also depletion of water in North Sahara and occurrence of large lake drainage areas.

GRACE data can be useful tool for drought monitoring. For example *Chew and Small* (2014) study an area in USA severely affected by drought in 2012 for more than two months. They used data from GRACE and 15 GNSS stations for period from 2006 to 2013 and compared it with hydrological and model data. They found that anomalies caused by the drought began in March 2012. Interestingly the minimum of TWS variations were found in summer 2013 i.e. more than a year after the drought. Differently from 2012 the soil moisture content in August 2013 was above average. This study finds that the TWS anomalies persisted for more than a year after that significant drought. In contrast, standard drought indices showed a more rapid recovery. According to *Zaitchik et al.* (2008) assimilation of GRACE data in models can contribute to large-scale drought monitoring. They analyse the water storage and fluxes in the Mississippi River basin using assimilation of GRACE data and independent measurements.

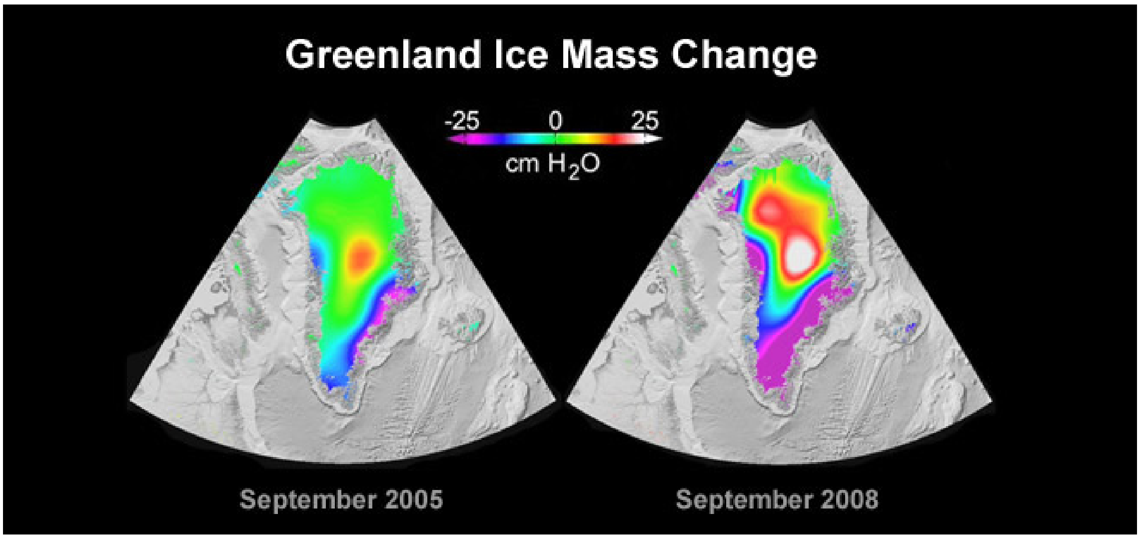

Figure 1.3: Greenland ice mass change, image credit: NASA/JPL.

GRACE can be used to study the losses from land ice and rising of the

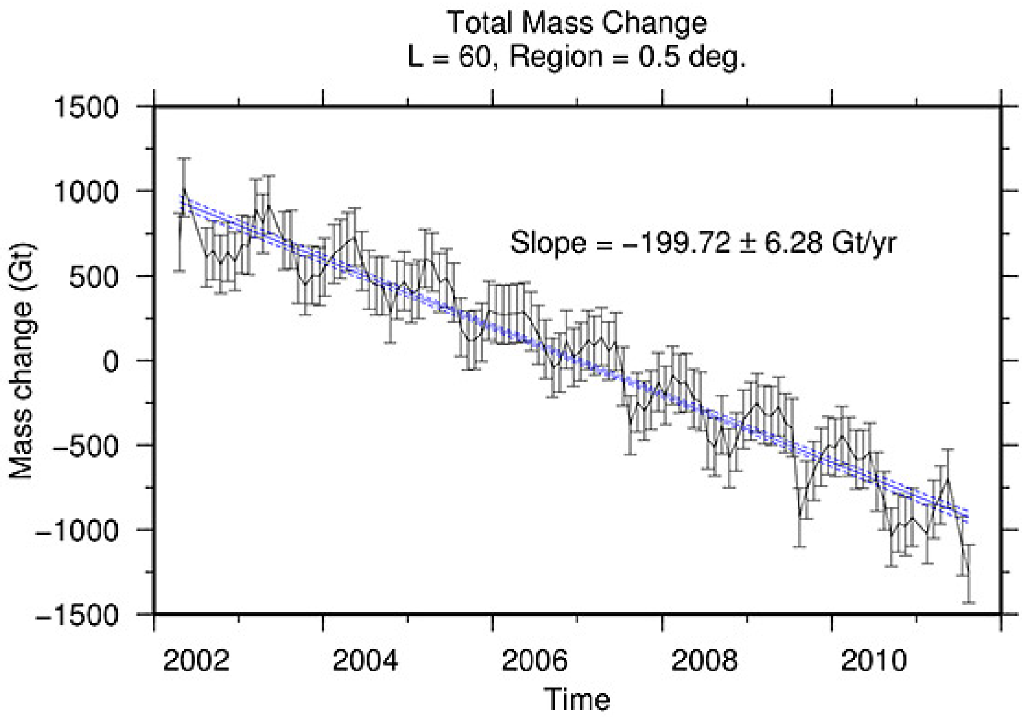

Figure 1.4: Greenland total ice mass change, after *Harig and Simons* (2012).

sea level. Figure 1.3 illustrates the changes in Greenland's ice mass as measured by GRACE and analysed by international researchers for the period between September 2005 (left) and September 2008 (right). The study is led by the Denmark National Space Institute in Copenhagen. The research indicates that the ice-loss acceleration began moving up the northwest coast of Greenland in late 2005. The team drew their conclusions by comparing data from GRACE with continuous GPS measurements made from long-term sites on bedrock on the edges of the ice sheet. Obviously apart of the losses there is increasing of the ice mass in the central area of Greenland. Figure 1.4 shows the amount of total mass change processed by Princeton researchers. The plot is extracted from *Harig and Simons* (2012) and shows that Greenland experienced a steady ice loss of 200 Gt annually*Gardner et al.* (2013) show that in many regions, local measurements give larger ice mass losses than satellite-based estimates. The largest mass losses for the 2003-2009 period form GRACE are in Arctic Canada, Alaska, coastal Greenland, the southern Andes, and high-mountain Asia, but there was little loss from glaciers in Antarctica. Over the research

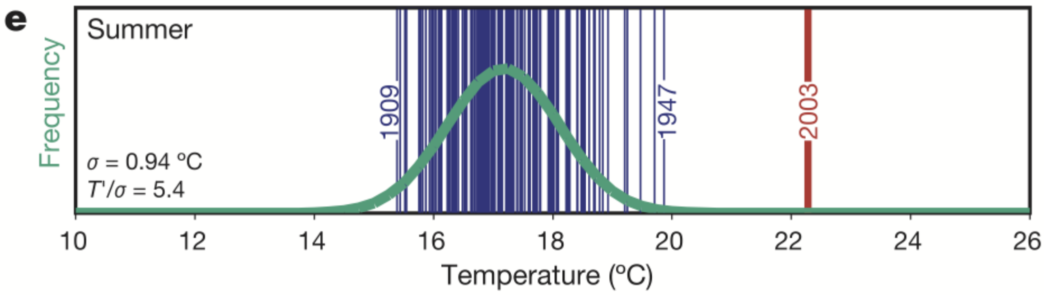

Figure 1.5: Distribution mean summer temperatures for 1864-2003 in Switzerland, after *Schär and Jendritzky* (2004).

period, the global mass budget was -259 ± 28 Gt per year, equivalent to the combined loss from both ice sheets and accounting for 29 ± 13 % of the observed sea level rise (2.50 ± 0.54 mm year^{-1}).

Observations of continental TWS anomaly has great importance for preventing the consequences of possible extreme events. Heat waves are example of such extreme events with large adverse social, economic and environmental effects that include increased mortality, transport restrictions and a decreased agricultural production. One of the widely studied European heat waves is August 2003. *Schär and Jendritzky* (2004) report mean summer temperature in Switzerland in 2003 on average 3° C higher than the 1961 - 90 mean. In the presented on figure 1.5 distribution of mean summer temperature in Switzerland for the period 1864-2003 the 2003 is clearly visible is an outlier. During the heat wave in many regions in Switzerland the annual precipitation deficit was 50 % below the average (*Ciais et al.*, 2005). The August 2003 heat wave represents a valuable benchmark case because regional climate model simulations suggest that by 2100 every second summer could be as warm or warmer and as dry or dryer. Figure 1.6 is from *Andersen et al.* (2005) and shows TWS variations for Central Europe during the 2003 heat wave. In this study measurements are compared for April-to-August period of 2002 and 2003 and the observed large negative anomaly in 2003 is associated with the heat wave. Validation of GRACE TWS with two independent hydrological estimates and direct gravity observations show agreement.

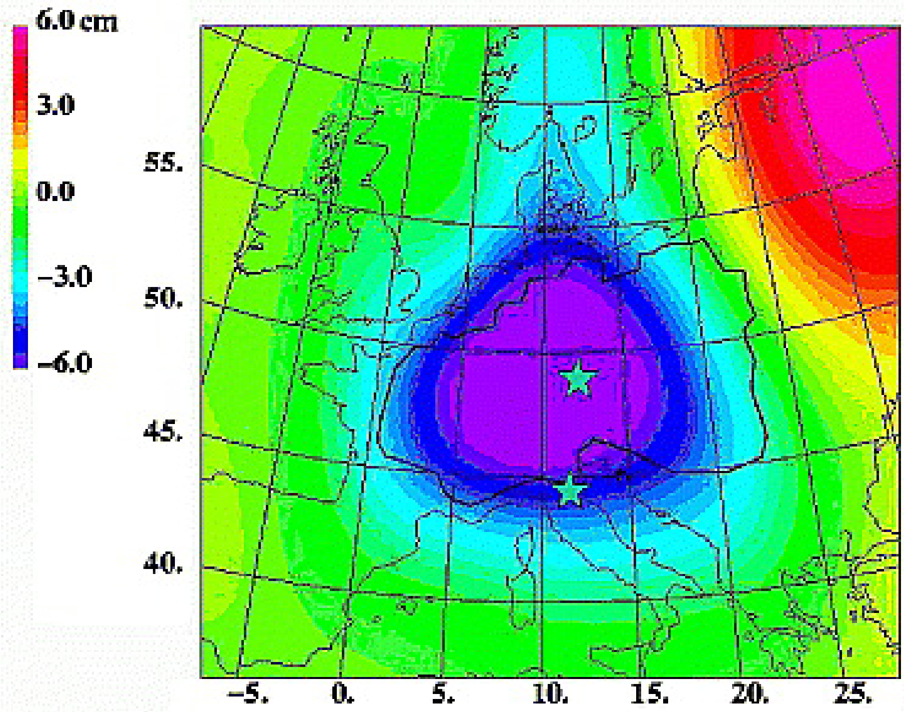

Figure 1.6: 2003 TWS anomaly for Central Europe, after *Andersen et al.* (2005).

Monitoring of water vapour and TWS is of interest in South-east Europe, since the heat waves are a common summer feature in the region. For example, the heat wave in July 2007 had large geographical extension reaching Bulgaria. The heat wave continued six days from 19 to 25 July. The atmospheric circulation leading to the heat wave is characterized by northerly displacement of the subtropical jet stream allowing the subtropical African air to reach the Balkan Peninsula as far as 50° N. On figure 1.7 is shown the air tongue spreading over the Mediterranean sea and Balkan Peninsula at 00 UTC on 23 July 2007.

The aim of this thesis is to investigate the anomalies of observed and modelled temperature, precipitation, IWV and TWS during the 2007 heat wave inSouth-east Europe. In chapter 2 are presented the data and the method used. Chapter 3 and 4 presents the 2007 anomalies of temperature, precipitation, IWV and TWS in observations and model, respectively. The conclusion

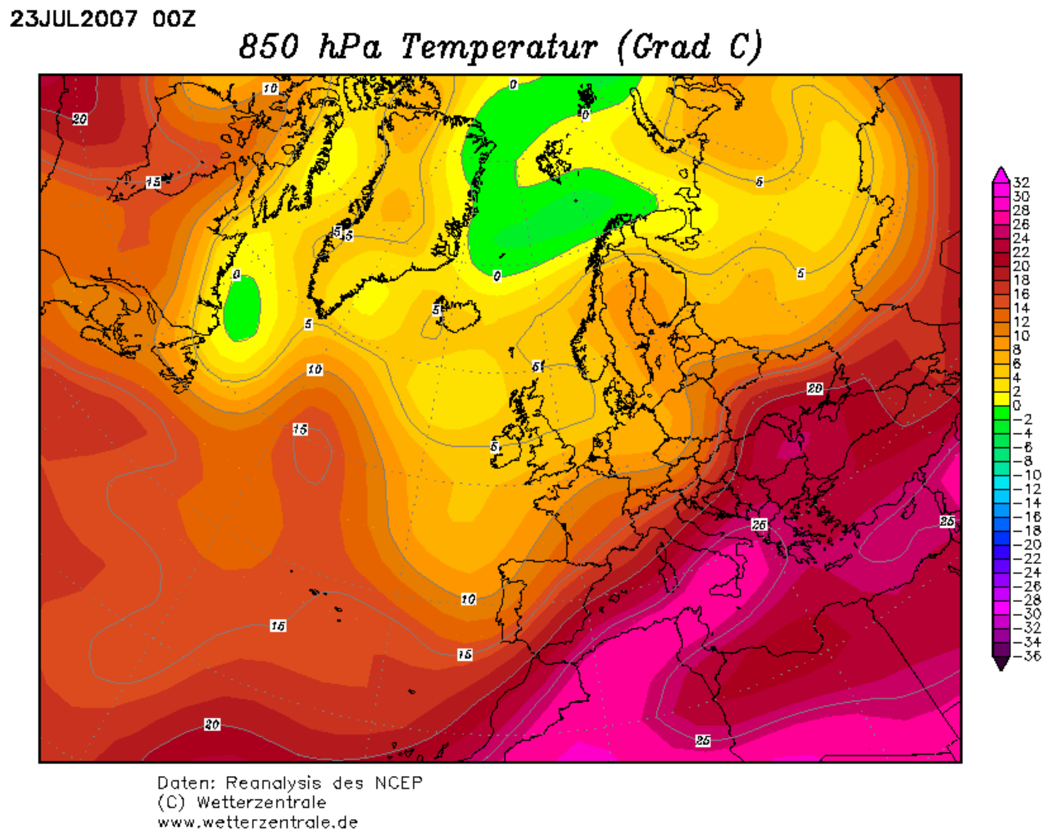

Figure 1.7: Temperature at 850 hPa (1.5 km msl.) on 23 July 2007 00 UTC., after *Simeonov et al.* (2013).

are given in Chapter 5.

Chapter 2

Data and methods

In this work are used surface and satellite observations in combination with simulations with a regional climate model ALADIN-Climate. The observation and simulations are archived in the Sofia University Atmospheric Data Archive (*Guerova et al.*, 2014). On figure 2.1 is shown the scheme of the data used in this work. The first column is for the ALADIN-Climate simulations described in section 2.4, the second is for the data flow of GNSS derived IWV (see section 2.3). It is to be noted that SYNOP observations (see the arrow in figure 2.1) are used to obtain GNSS IWV. The surface observations from synoptic station (SYNOP) are in column three (see section 2.2) and the GRACE data set is in column four (see section 2.1).

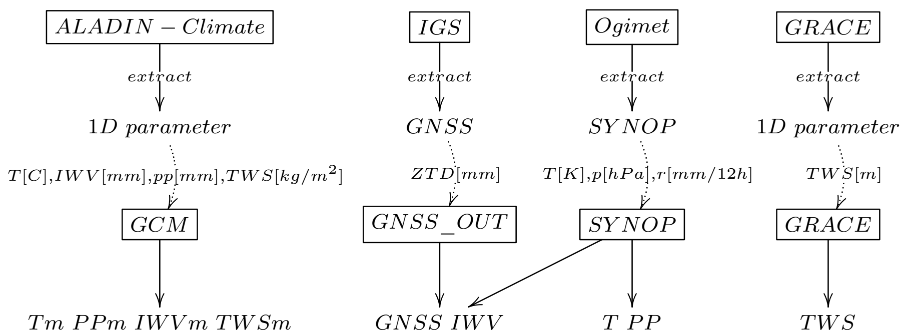

Figure 2.1: SUADA table names and data flow used in this thesis.

2.1 GRACE data

GRACE satellite mission is a cooperation between the National Aeronautics and Space Administration (NASA) and the German Research Centre for Geosciences (GFZ). GRACE mission is of two identical satellites that fly 220 km apart on a polar orbit at 500 km above surface. Figure 2.2 illustrates the GRACE twin satellite connected with highly precise K-band microwave system which measures the gravity anomaly as a change in the distance between the satellites. Such variations in the distance between the satellites are possible when the lead spacecraft passes above large concentration of mass i.e. a stronger gravity pulls it away from the second GRACE satellite behind in the same orbital plane. These measurements, along with GNSS based location information are used to compute monthly gravity field solutions (web, d).

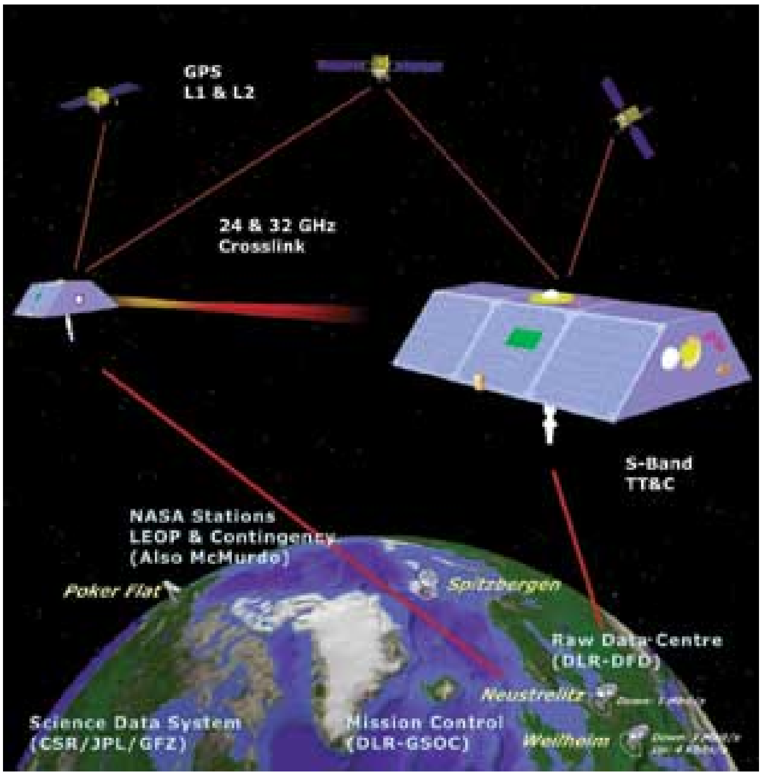

Figure 2.2: GRACE mission - twin satellites on polar orbit (500 km) connected with laser link, image credit: web (a).

In figure 2.3 is presented the GRACE processing scheme. The satellite orbits are processed in daily arcs. For each arc initial conditions, stochastic accelerations and accelerometer scale factors are estimated (Level 1 data). The spherical harmonic coefficients of the gravity field are set up together with the arc-specific parameters. The daily Normal EQuations (NEQs) with respect to the kinematic orbits of GRACE satellites and with respect to the K-Band range-rate observations are combined and the arc-specific parameters are pre-eliminated from the combined NEQs. Finally the reduced NEQs are accumulated to monthly batches to solve for the gravity model parameters. The result are mathematical functions defined on surface of a sphere - spherical harmonics, which solutions are spherical harmonic coefficients. GRACE coefficients are objective mainly for continental water storage (Level 2 data), but also include errors from the correction models and noise (*Swenson and Wahr*, 2006).

The temporal variations of the gravity filed over the continents are attributed to: 1) the hydrological cycle, 2) ice mass changes in the polar, subpolar regions and large glaciers, and 3) post glacial rebound. Using a priori models of known gravitational accelerations the static gravity field of the Earth, which represents 99 % of the observed signal, its time variations are removed. Polar movements, atmosphere and ocean mass changes also are removed in order to analyse the continental hydrology component of water storage. For this purpose are used global ocean circulation models and reanalysis from European Centre for Medium-Range Weather Forecasts (ECMWF) and National Centres for Environmental Prediction (NCEP).

In this study is used GRACE Level 2 monthly gravity variations, represented in equivalent water height. The variations were computed from GRACE satellite observations and derived from Astronomical Institute at University of Bern (AIUB-RL02) series of monthly gravity fields (*Meyer et al.*, 2016). Values are calculated within a radius of 300, 500 and 700 km around Sofia. A Gaussian bell curve was applied for weighting. The radius given is the half width radius of the Gaussian bell curve, which is a common procedure for smoothing of GRACE derived gravity models.

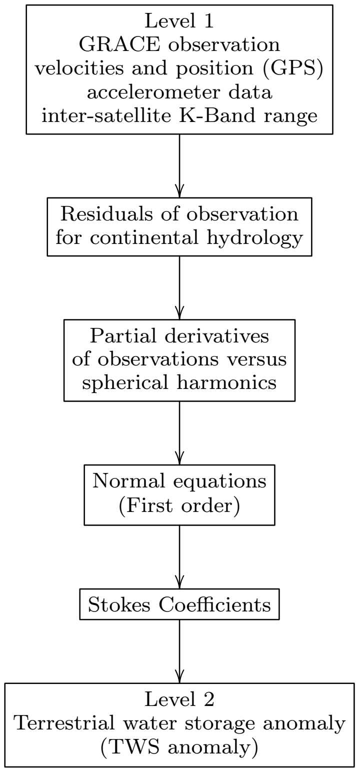

Figure 2.3: GRACE processing scheme for TWS derivation.

2.2 Surface synoptic data

In this thesis are used surface synoptic observations (SYNOP) of temperature and precipitation from Sofia station of the National Institute of Meteorology and Hydrology (NIMH). The data is acquired from OGIMET, which is an on-line weather information server, and is uploaded in SUADA. Data is placed at SYNOP table of the database. The SYNOP table contains unprocessed meteorological data. The surface temperature (T) and precipitation (PP) are extracted from SUADA and monthly mean time series and anomalies are computed using MATLAB and R programs. Errors of the observation are $\pm$ 0.1° C for temperature and $\pm$ 0.5 mm for precipitation.

2.3 GNSS tropospheric products

The GNSS tropospheric products are from the first processing campaign of the International GNSS Service (IGS) (*Byun and Bar-Sever*, 2009; *Rebischung et al.*, 2012). IGS is a scientific consortium from over 200 worldwide national agencies, universities and research institutions from more than 80 countries. It computes and maintains a global network of over 350 permanent, continuously operated GNSS sites. IGS provides data for total tropospheric delay in zenith direction (ZTD). The GNSS station in Sofia (SOFI) is processed since 1997. The SUADA contains continuous GNSS data for SOFI from 1997 to 2015. To derive IWV from the ZTD the 2 meter surface pressure (p_s) and temperature (t_s) from SYNOP are used as bellow:

$$ZWD = ZTD - 2.2768 \frac{p_s}{1 - 0.00266 cos(2\theta) - 0.00028 h} \tag{2.1}$$

$$IWV = \frac{10^6}{(k_3/T_m + k_2) R_v} ZWD, \tag{2.2}$$

where k_2, k_3 and R_v are constant, T_m is the weighted mean atmospheric temperature, h is the height and θ is the latitude variation of the gravitational acceleration.

After computing the IWV values they are stored in GNSS_OUT table of SUADA. Errors of the GNSS IWV are less than 1 mm.

2.4 Regional climate model ALADIN-Climate

ALADIN-Climate is a Regional Climate Model (RCM) developed in an international cooperation at Mètèo France. It was created merging the dynamics of the numerical weather prediction model ALADIN and the parameterization schemes from ARPEGE-Climate global climate model. The currently used version of ALADIN-Climate is described in *Csima and Horányi* (2008). ALADIN-Climate parameterization schemes include: 1) Fouquart and Morcrette radiation scheme (*Morcrette*, 1989), 2) ISBA land scheme (*Noilhan and*

Planton, 1989) of four layers of soil temperature without a deep relaxation, two soil moisture layers (with parameterization of soil freezing) and a single layer snow model (with variable albedo and density), based on *Douville et al.* (1995), 3) deep convection scheme designed according to *Bougeault* (1985), 4) cloud scheme by *Ricard and Royer* (1993), and 5) large-scale precipitation scheme following *Smith* (1990). Lateral boundary conditions for ALADIN-Climate simulation are from ERA-Interim reanalysis developed at ECMWF and described in (*Dee et al.*, 2011). The RCM is integrated over the EURO-CORDEX domain presented in figure 2.4 for the hindcast period of 1989-2008. ALADIN-Climate spatial resolution is 50 km (0.44°) with 31 vertical levels.

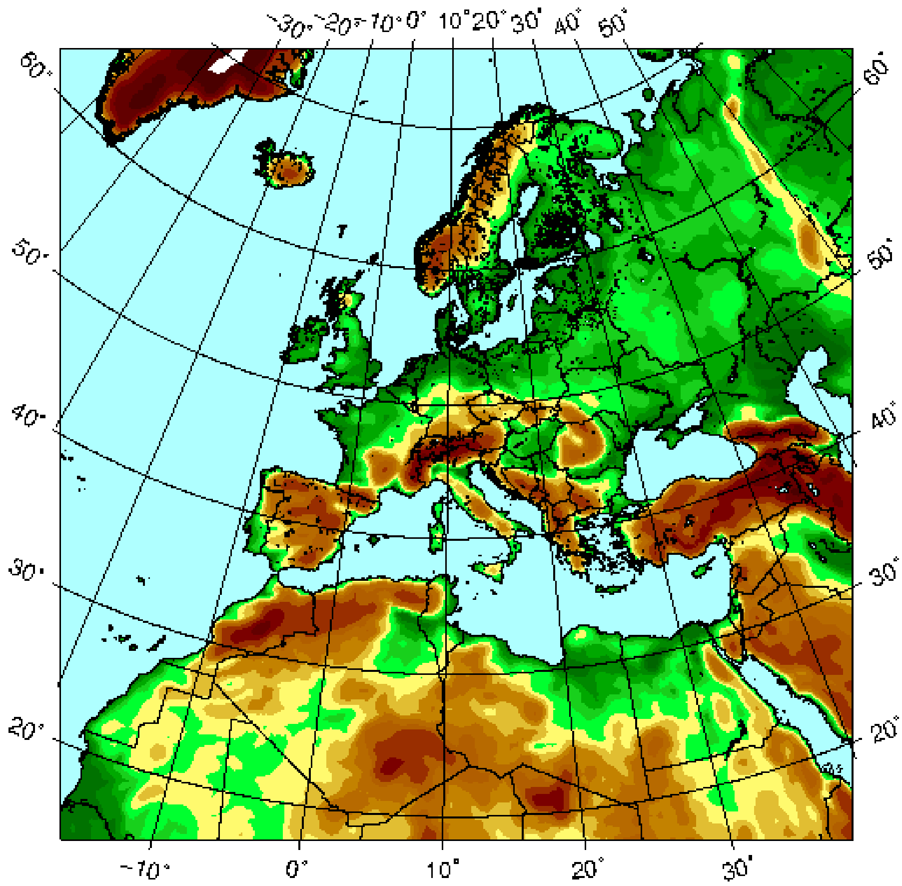

Figure 2.4: ALADIN-Climate RCM domain.

In this work ALADIN-Climate data are used for the period 2003-2008 since it is the only common set with the observations. Data is achieved in

SUADA database in table GCM. Extracted is one model grid point with latitude 42° 25' N, longitude 23° 25' E and altitude 1130 m asl. In table 2.1 are shown ALADIN-Climate model coordinates and those of SYNOP station Sofia and GNSS station SOFI.

Station name	longitude (East)	latitude (North)	altitude (m asl)
SYNOP-Sofia	23° 35'	42° 41'	590
GNSS-SOFI	23° 25'	42° 29'	1120
ALADIN-Cl.	23° 25'	42° 25'	1130

Table 2.1: Coordinates of observation and model grid point.

Chapter 3

Observation anomalies: 2007 vs 2003-2013

In this section observations from SYNOP, GNSS and GRACE are presented for period 2003-2013.

3.1 Temperature and precipitation anomaly from observations

On figure 3.1 a, b, c, d are shown: 1) monthly mean temperatures time series, 2) moving average of length 6, 3) monthly mean temperatures for 2007 compared with period 2003-2013, and 4) monthly anomalies for 2007. As can be seen from figure 3.1a the temperature has an annual cycle. The peak is in summer months - June, July and August and minimum is in winter time - December and January. On figure 3.1b is filtered data by moving average of length 6. By this filter are smoothed high frequency variations and is reduced the effect of all cycles with periods smaller or equal to six months. Clearly seen is the steady increase of temperature trend in the summer of 2007. When compared to 2003-2013 mean (3.1c, dashed line), it is obvious that temperature in first 8 months of 2007 are higher. Next months to the end of 2007 the temperature is lower than the 2003-2013 monthly means. From figure 3.1d is seen that the temperature anomaly in July 2007 is positive - 2.3° C above 2003-2013 mean. Interestingly the largest positive anomaly is in January - almost 5.4° C above the 2003-2013 mean.

Figure 3.2 presents: 1) precipitation time series, 2) moving average of length 6, 3) monthly mean precipitation for 2007 compared with period 2003-2013, and 4) precipitation anomaly for 2007. According to figure 3.2a precipitation time series do not show annual cycle. There are more than one peak per year. Maximums of precipitation appear in the end of spring (May, early summer June) and autumn (September and October), although there are some exceptions. In 2005 the peaks are in winter (December) and summer (August). In 2009 again precipitation maximums appears in winter (January) and summer time (August). Winter maximum can be seen again in December 2010, January 2012 and February 2013. Most of the minimums can be noticed in spring (Mart and April) and in the end of autumn (November). Significant minimums in the end of winter and early spring are obtained in February 2008 and 2009 and in March 2003 and 2012. Large summer minimums are seen only in August 2003, July 2007 and August 2008. In summary this figure shows the irregular behaviour of precipitation, but it can be said that the large peaks are slowly moved from early spring and autumn to winter and summer, respectively. In addition it can be seen that the amplitude of peaks becomes smaller over time. This is confirmed in figure 3.2b. The filtered data of precipitation show decrease after 2006. At figure 3.2c is shown monthly mean precipitation for 2007 (white bars) and 2003-2013 (green bars). Maximum for 2003-2013 monthly mean precipitation is 85 mm in June with a minimum of 30 mm in November. In 2007 the monthly mean precipitation reaches 175 mm in May and 5 mm in July. The anomalies are plotted in figure 3.2d. In July 2007 precipitation anomaly reached -60 mm - the absolute minimum for this year. In January 2007 the precipitation is in the norm.

3.2 IWV anomaly from observations

On figure 3.3a, b, c, d are shown: 1) monthly mean IWV time series, 2) moving average of length 6, 3) monthly mean IWV for 2007 and 2003-2013 and 4) monthly anomalies for 2007, respectively. From 3.3a is seen that, similar to the temperature, monthly mean IWV has annual cycle. Each year starts with upward trend and peaks in summer (June, July or August) followed by downward trend and minimum in winter season (December, January or February). Also according to 3.3a the minimums as well as the maximums of IWV increase their amplitude almost each following year. On figure 3.3b is shown the IWV moving average with length 6. As it can be seen the lowest IWV values are in the end of 2006 and the beginning of 2007. Large maximum is recorded in summer 2009. On figure 3.3c is shown the monthly mean IWV values for 2007 (thick line) versus 2003-2013 (dashed line). In first four months of 2007 IWV is constant then increases in May. Clearly IWV in July 2007 is smaller than 2003-2013. Until the end of 2007 IWV is below or close to the norm. On figure 3.3d is plotted the IWV anomaly and the first negative anomaly is in April followed by July, September and December. Positive anomaly in May is 2 mm above the mean for 2003-2013 period. The largest negative anomaly is in July and is 3.5 mm under the norm.

3.3 TWS anomaly from observations

Figure 3.4 a, b, c, d shows: 1) TWS anomaly time series, 2) moving average by length 6, 3) monthly mean TWS anomalies and, and 4) 2007 anomaly. On figure 3.4a is shown TWS variations in centimetres for ten year period from 2003 to 2013 for 3 smoothing radii - 300 km (R1 - black line), 500 km (R2 - red line), and 700 km (R3 - blue line). As can be seen the TWS variations have annual cycle. Each year starts with upward trend of TWS anomaly and after passing its peak in February, March or April a downward trend leads to the minimum in August, September or October. Then in next months TWS starts to increase again. What differs every year is the amplitude of TWS anomaly. Also the maximums and minimums are indicative for significant changes in some of the water cycle components. For example the minimum of more than -15 cm (for R1) in the TWS anomaly trend that appears in 2003 is likely linked to the heat wave occurred in Europe. Second lowest magnitude of TWS variations is noticed in summer of 2007. In August, a month after appearance of Balkan heat wave TWS value reached -10 cm. On figure 3.4b is seen moving average of length 6 for GRACE data using only the radius of 300 km. Clearly seen is the negative TWS trend in summer months of 2007. The largest negative TWS anomaly is also in summer 2007 (figure 3.4c). In August 2007 TWS anomaly has a minimum of -10 cm. All months in 2007, with exception of November and December, have negative TWS anomaly or are close to the mean.

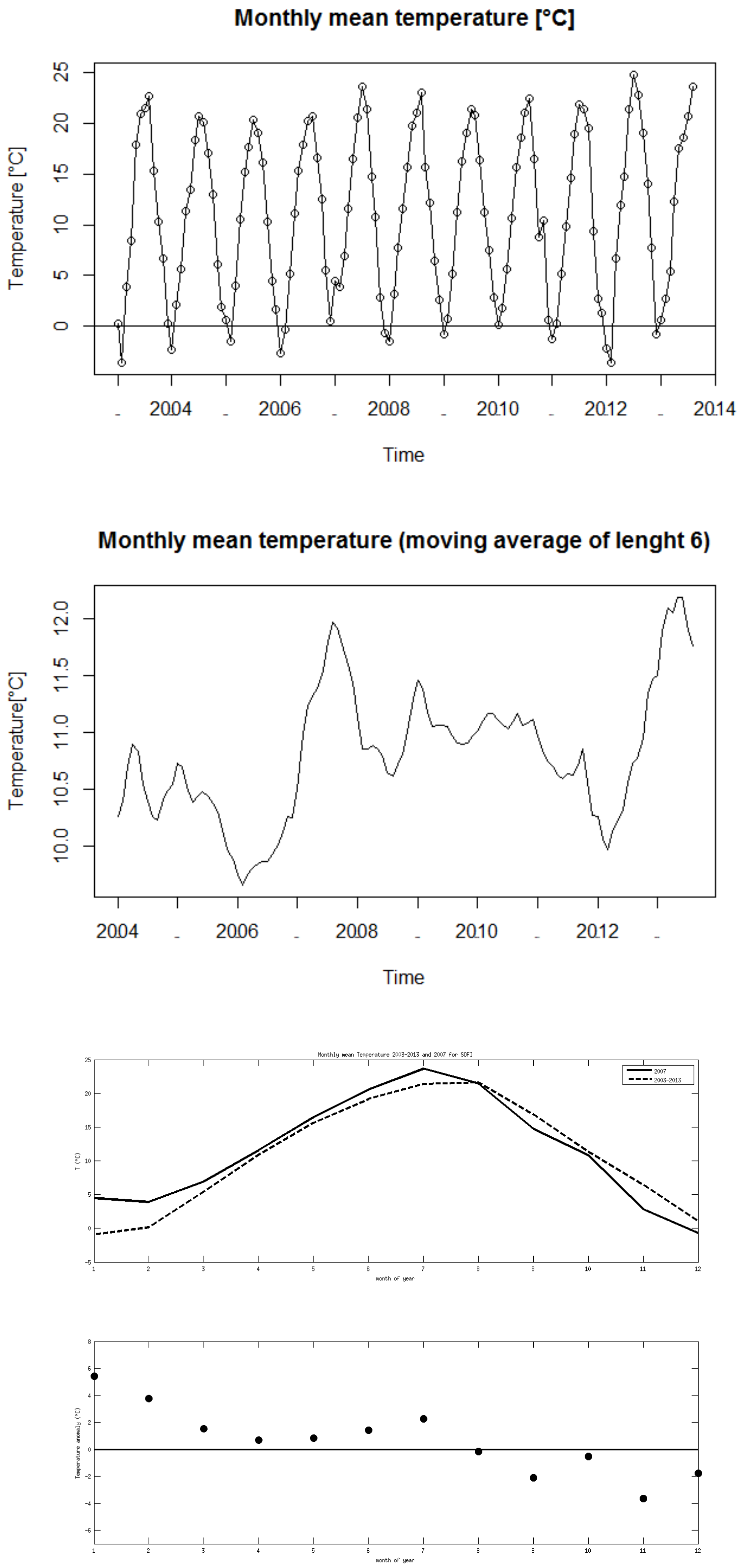

Figure 3.1: (a) Temperature time series for period 2003-2013; (b) moving average of length 6; (c) monthly mean temperatures for 2003-2013 (dashed line) and for 2007 (thick line); (d) anomalies for 2007 versus 2003-2013.

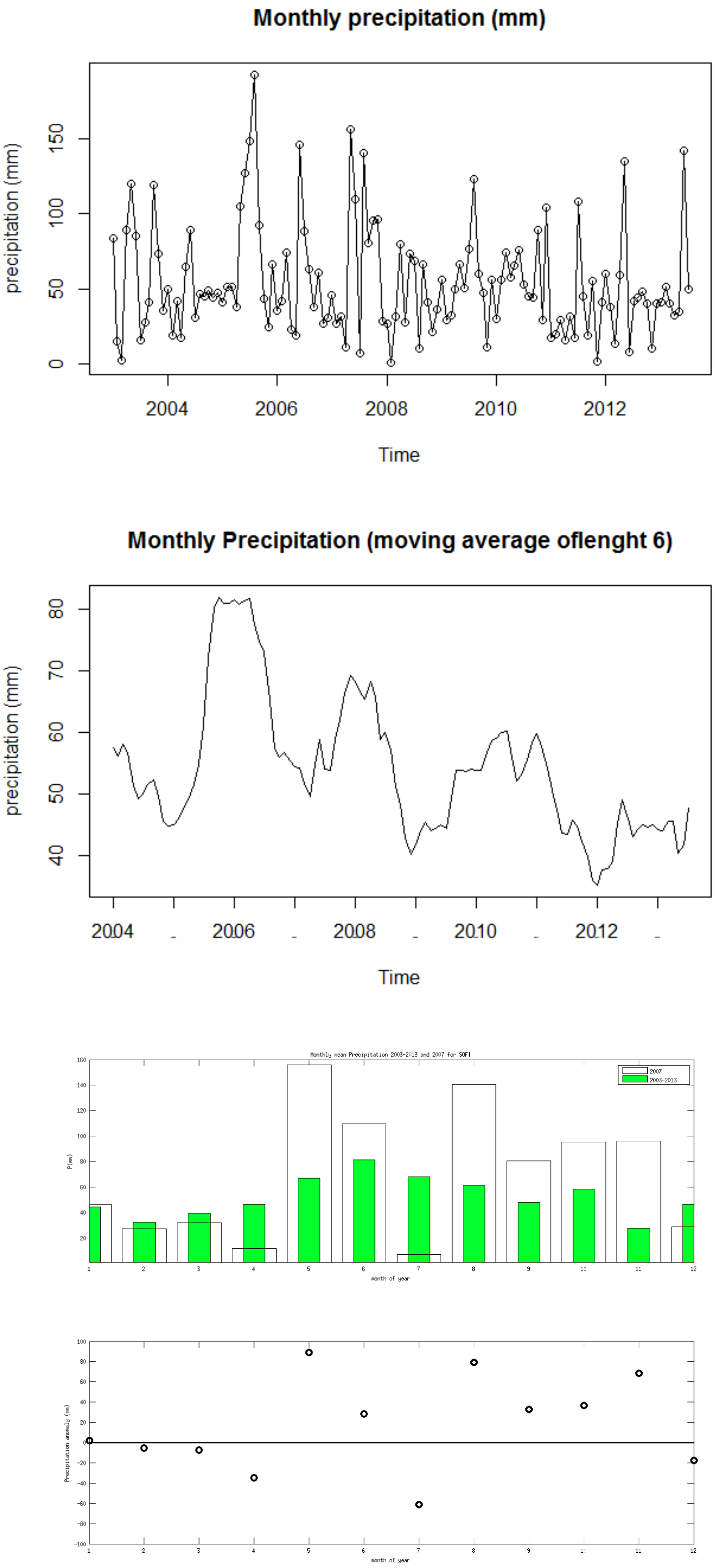

Figure 3.2: (a) Precipitation time series for period 2003-2013; (b) moving average of length 6; (c) monthly mean precipitation for 2003-2013 (dashed line) and for 2007 (thick line); (d) precipitation anomalies for 2007 versus 2003-2013.

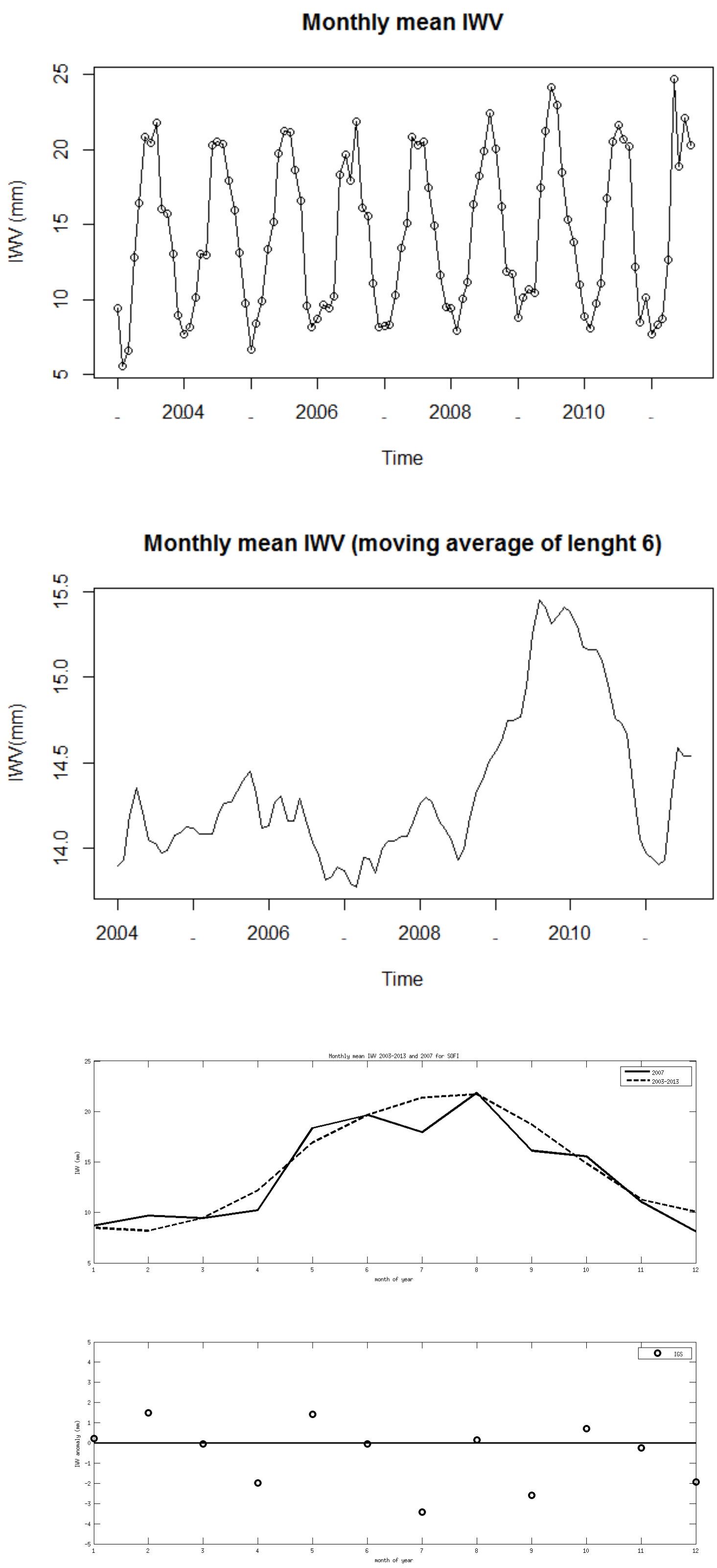

Figure 3.3: (a) IWV time series for period 2003-2013; (b) moving average of length 6; (c) monthly mean IWV for 2003-2013 (dashed line) and for 2007 (thick line); (d) IWV anomalies for 2007 versus 2003-2013.

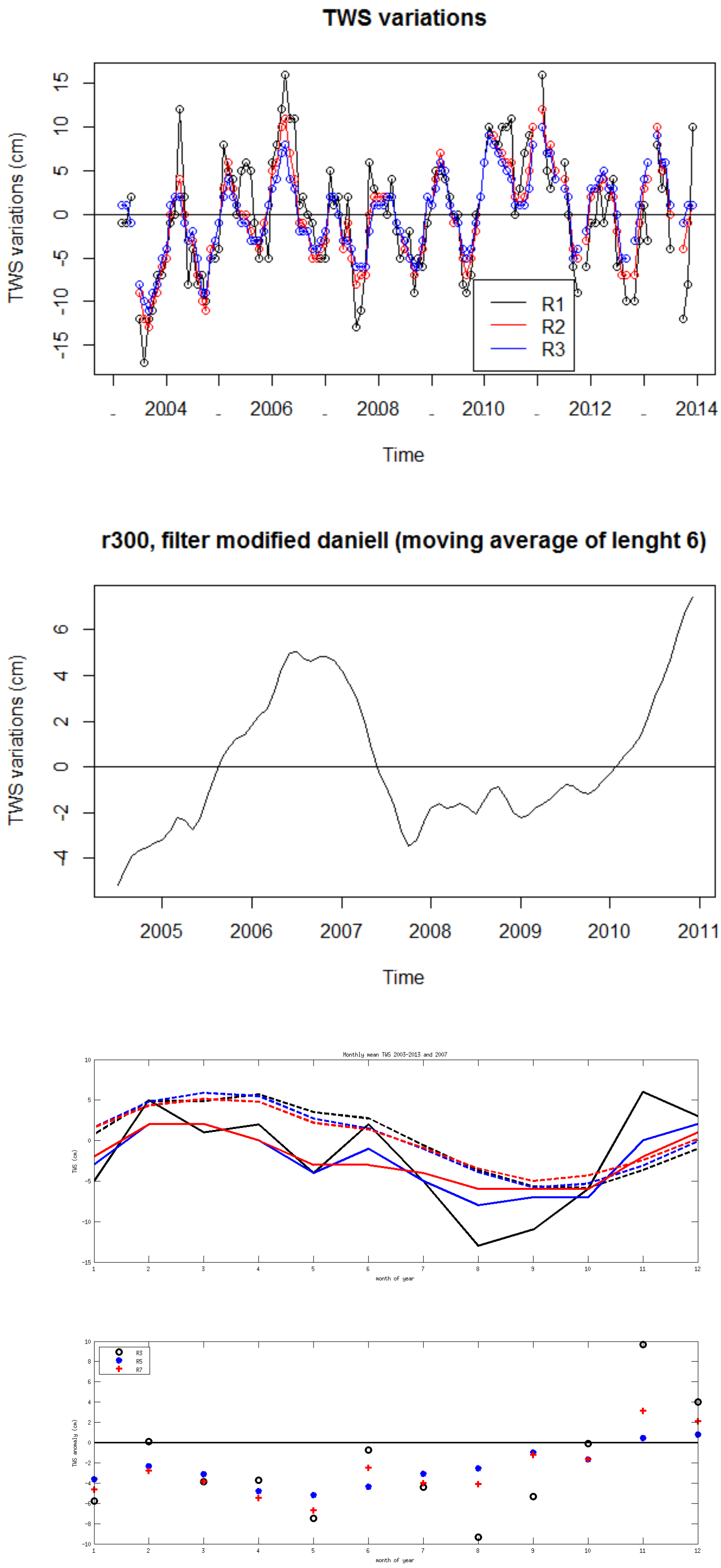

Figure 3.4: (a) TWS variations time series for period 2003-2013 with smoothing radii of 300 km (R1 - black line), 500 km (R2 - red line) and 700 km (R3 - blue line); (b) moving average of length 6; (c) monthly mean TWS changes for 2003-2013 (dashed line) and for 2007 (thick line); (d) TWS anomalies for 2007 versus 2003-2013.

Chapter 4

RCM anomalies: 2007 vs 2003-2008

In this section observations from SYNOP, GNSS and GRACE are compared with ALADIN-Climate model simulations. All data is processed for period 2003-2008. On plots are presented monthly anomalies in 2007 when compared to 2003-2008, for both observation and model. Correlation coefficient of temperature, precipitation, IWV and TWS pairs is given in table 3.2.

4.1 Temperature and precipitation anomaly RCM

At figure 4.1a are shown monthly temperature anomalies for 2007 from SYNOP observation (black circles) and ALADIN-Climate model (red circles). In the SYNOP data first eight months of 2007 are with positive temperature anomaly and the remaining four are with negative. Large positive anomaly occurs in January - above 5° C. In July the anomaly reaches up to 3° C. Only one difference in ALADIN-Climate model is seen with a negative anomaly in April. The month with highest temperature anomaly (5° C) in ALADIN-Climate is in June. When compared the result the following features stand out: 1) large positive temperature anomaly in January, 2) positive anomaly in July, and 3) large negative anomaly in November. The model data results are in good agreement with SYNOP observations and correlation is 0.70.

On figure 4.1b are shown monthly precipitation anomalies for 2007. When compared the following features stand out: 1) in first quarter (January-March) precipitation anomalies are in good agreement and the amplitude differences are in the range of 10 mm, 2) in the next quarter the precipitation anomalies have big discrepancy, 3) both data sets have negative anomaly in July, and 4) precipitation anomalies are in agreement for the next months with exception of September. Here the mismatches are more than the coincidences, although in July precipitation anomaly is negative and then is positive in August in both observation and RCM. Correlation coefficient for precipitation anomaly data pair is 0.32, which indicates poor agreement.

4.2 IWV anomaly RCM

Monthly IWV anomalies are shown on figure 4.2 Again two methods are compared - GNSS data from station SOFI (black circles) and ALADIN-Climate model (red circles). When compared results the following features stand out for 2007: 1) positive IWV anomaly in February, 2) negative IWV anomaly in April, and 3) negative IWV anomaly in July. According to GNSS data the minimum value of IWV anomaly is in July(- 3 mm), while for the model minimum is in September (-2 mm). The correlation coefficient of 0.73 suggests strong relation between GNSS and RCM.

4.3 TWS anomaly RCM

Monthly TWS anomalies from GRACE (black circles) and ALADIN-Climate model (red circles) are shown on figure 4.3 When compared the following features stand out for 2007: 1) downward trend of TWS anomaly from February to May, 2) TWS is in range of 1 cm in June, and 3) large differences in the second half of the year after June. There is not a good agreement between the data. That is confirm from the correlation coefficient of -0.68. Although the

year/corr	T	P	IWV	TWS
2007	0.70	0.32	0.73	-0.68

Table 4.1: Correlation coefficient of 2007 anomalies of temperature (T), precipitation (PP), IWV and TWS.

month	T Tm	PP PPm	IWV IWVm	TWS TWSm
J	+ +	0 -	+ +	- +
F	+ +	0 +	+ +	+ +
M	+ +	- -	+ -	- +
A	+ -	- +	- -	- 0
M	+ +	+ -	+ +	- +
J	+ +	+ -	0 -	+ +
J	+ +	- -	- -	- +
A	+ +	+ +	0 +	- +
S	- -	+ -	- -	- -
O	- -	+ +	+ +	+ -
N	- -	+ +	- -	+ -
D	- -	- -	- -	+ -

Table 4.2: Observation and model anomalies for 2007 versus 2003-2008.

value of the coefficient is high the negative sign shows that if the one variable moves higher or lower the other moves in the opposite direction with close magnitude.

On table 3.1 are shown the correlation coefficients of monthly mean anomalies in 2007 observations and RCM. As it can be seen temperature and IWV anomalies have strong positive relation. The same can not be said for the relation between the precipitation data. It seems like in many cases the precipitation and TWS amount is underestimated by the model. The negative correlation in case of TWS anomalies shows that there is an uncertainties with determination of the model TWS variations.

In table 3.2 are shown all anomalies for 2007 by observational SYNOP (T, PP), GNSS (IWV), GRACE (TWS) and ALADIN-Climate model (Tm, PPm, IWVm, TWSm). Red colour indicates the extremums both minimums (-) and maximums (+). In confirmation with the correlation coefficients from table 3.1, there is a good agreement between the SYNOP and ALADIN-Climate model as well as between the GNSS and RCM. The negative correlation between GRACE and ALADIN-Climate is also confirmed by this table. Obviously in almost each month the direction of GRACE TWS anomaly is opposite from the model results.

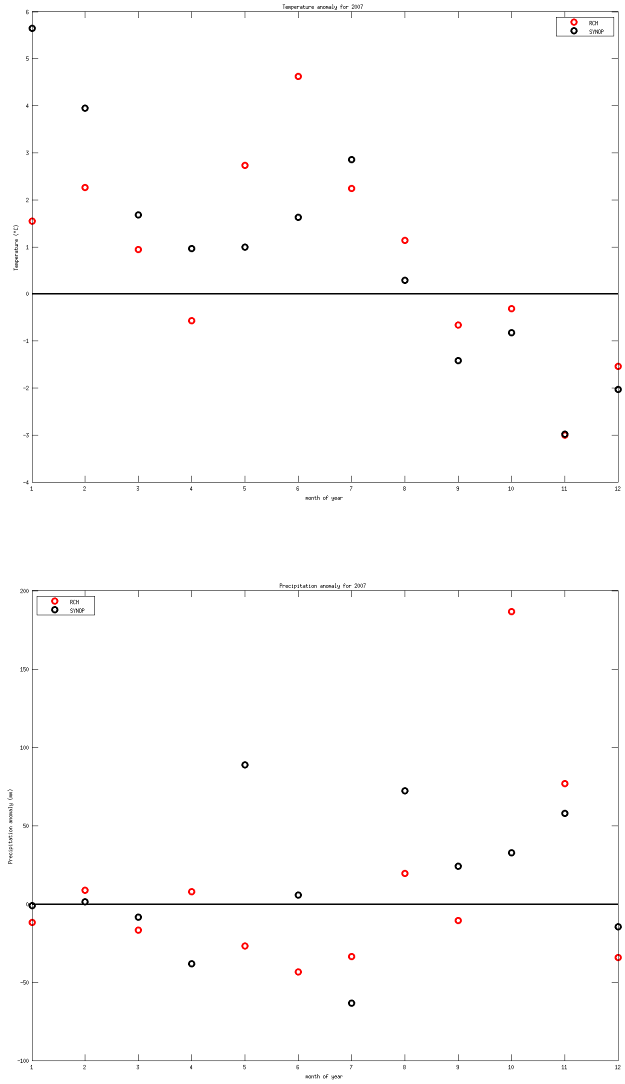

Figure 4.1: Temperature (top) and precipitation anomalies (bottom) for 2007 from SYNOP observations (black circles) and ALADIN-Climate model (red circles).

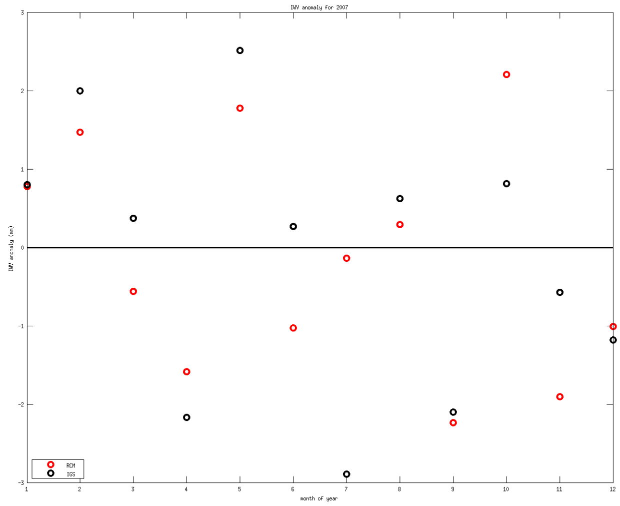

Figure 4.2: IWV anomaly for 2007 from observations (black circles) and ALADIN-Climate model (red circles).

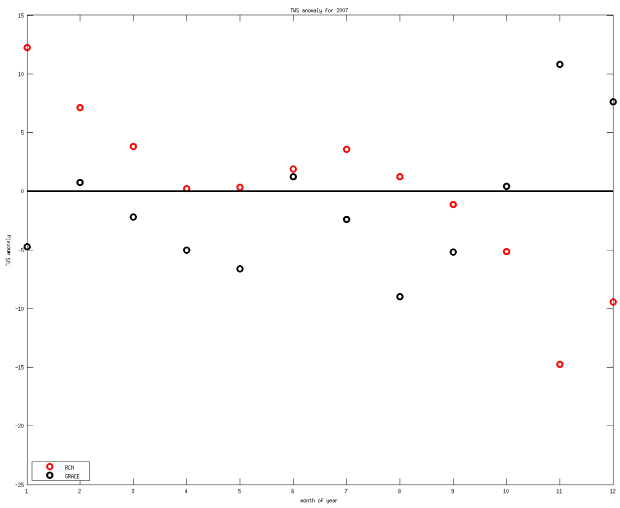

Figure 4.3: TWS anomaly for 2007 from observations (black circles) and ALADIN-Climate model (red circles).

Chapter 5

Conclusions

In this thesis the synergy between surface and satellite observations is used to study the behaviour of three components of the hydrology cycle namely, precipitation, water vapour and terrestrial water storage during the July 2007 heat wave in South-east Europe. The e anomalies of temperature, precipitation, IWV and TWS in 2007 as compared to 2003-2013 indicate relation between them and the occurrence of the heat wave in July. Surface observations show positive temperature anomalies for first eight months of 2007. The heat wave month (July 2007) was 2° C hotter than the 2003-2013 mean in Sofia, Bulgaria. There are significant negative precipitation anomalies in March, April and July 2007. According to GNSS data the minimum of IWV is in July 2007. GRACE data is in good agreement with the surface and GNSS results and show minimums in spring and summer. The absolute minimum of TWS anomaly is in August i.e. a month after the occurrence of the heat wave, possibly due to the slower response of the soil to the heating.

In addition the observed anomalies in 2007 are compared to simulations with the regional climate model ALADIN-Climate. The comparison between anomalies from observations and ALADIN-Climate model gives: 1) strong correlation for temperature and IWV between the two data sets, and 2) weak relation between the precipitation and TWS anomalies data set. The comparison shows that the precipitation and TWS amount tend to be underestimated in the model. Precipitation and terrestrial water storage are very difficult to simulate thus assimilation of GRACE observations in the climate model can be a possible way to correct this deficiency.

The result of using GRACE data shows that there is strong capacities of multi-satellite observations to monitor quantitatively the changes in the storage of surface and sub-surface reservoirs associated with climate variability and human activities at a regional scale. In the near future the remotely sensed data sets like GRACE are likely to have large impact in regions like Bulgaria where in situ data are sparse. University of Bern is currently coordinating a project aiming to set European Gravity Service for Improved Emergency Management (EGSIEM, *Jaeggi* (2015)). EGSIEM objectives are: 1) to deliver the best time-variable gravity products for applications in Earth and environmental science research, 2) to reduce the latency and to increase the temporal resolution of the gravity and related mass redistribution products, and 3) to develop gravity-based indicators for extreme hydrological events and demonstrate their value for flood and drought forecasting and monitoring services. Primary input to EGSIEM is the GRACE and GRACE-FO (Follow-on, NASA-GFZ, due for launch in 2017) satellite mission data.

Acknowledgement

I would like to thank to:

- Assoc. prof. Guergana Guerova for being my thesis supervisor and helping me during my study.

- Tzvetan Simeonov for his help with operating SUADA and GNSS processing.

- Dr. Ulrich Meyer, from the University of Bern for providing GRACE data.

- Peter Szabo from the Hungarian Meteorological Service for providing ALADIN-Climate data.

Bibliography

University of Texas at Austin center for space research, `http://csr.utexas.edu/grace/publications/brochure/page11.html`, a.

Global terrestrial observation system, `http://www.fao.org/gtos/gt-nethyd.html`, b.

Global TWS anomaly, `http://www.globalwaterforum.org/wp-content/uploads/2013/08/Figure-3.png`, c.

Gravity Recovery And Experiment, `http://nasa.gov/Grace`, d.

GRACE Follow-On, `http://gracefo.jpl.nasa.gov`, e.

Andersen, O. B., S. I. Seneviratne, J. Hinderer, and P. Viterb, GRACE-derived terrestrial water storage depletion associated with the 2003 European heat wave, *Geophysical research letters*, *32*, L18,405, doi:10.1029/2005GL023574, 2005.

Bougeault, P., A simple parameterization of the large-scale effects of cumulus convection, *Monthly Weather Review*, *113*(12), 2108–2121, 1985.

Byun, S. H., and Y. E. Bar-Sever, A new type of troposphere zenith path delay product of the international GNSS service, *Journal of Geodesy*, *83*(3-4), 1–7, 2009.

Chew, C. C., and E. E. Small, Terrestrial water storage response to the 2012 drought estimated from GPS vertical position anomalies, 2014.

Ciais, P., et al., Europe-wide reduction in primary productivity caused by the heat and drought in 2003, *Nature*, *437*(7058), 529–533, 2005.

Csima, G., and A. Horányi, Validation of the ALADIN-Climate regional climate model at the Hungarian meteorological service, *Időjárás*, *112*(3-4), 155–177, 2008.

Dai, A., Recent climatology, variability, and trends in global surface humidity, *Journal of Climate*, *19*(15), 3589–3606, 2006.

Dee, D., et al., The ERA-Interim reanalysis: Configuration and performance of the data assimilation system, *Quarterly Journal of the Royal Meteorological Society*, *137*(656), 553–597, 2011.

Douville, H., J.-F. Royer, and J.-F. Mahfouf, A new snow parameterization for the Meteo-France climate model, *Climate Dynamics*, *12*(1), 21–35, 1995.

Gardner, A. S., G. Moholdt, J. G. Cogley, B. Wouters, and F. Paul, A reconciled estimate of glacier contributions to sea level rise: 2003 to 2009, *Science*, *304*, 852–857, 2013.

Guerova, G., T. Simeonov, and N. Yordanova, The sofia university atmospheric data archive (suada), *Atmospheric Measurement Techniques*, *7*(8), 2683–2694, 2014.

Harig, C., and F. J. Simons, Mapping Greenland's mass loss in space and time, *Proceedings of the National Academy of Sciences*, *109*(49), 19,934–19,937, 2012.

Jaeggi, A., European gravity service for improved emergency management-project overview and first results, in *2015 AGU Fall Meeting*, Agu, 2015.

Matzarakis, A., C. De Freitas, and D. Scott, Developments in tourism climatology, in *3rd International Workshop on Climate, Tourism and Recreation, Freiburg*, Citeseer, 2007.

Meyer, U., A. Jäggi, Y. Jean, and G. Beutler, AIUB-RL02: an improved time series of monthly gravity fields from GRACE data, *Geophysical Journal International*, p. ggw081, 2016.

Morcrette, J.-J., *Description of the radiation scheme in the ECMWF model*, European Centre for Medium-Range Weather Forecasts, 1989.

Noilhan, J., and S. Planton, A simple parameterization of land surface processes for meteorological models, *Monthly Weather Review*, *117*(3), 536–549, 1989.

Ramillien, G., F. Frappart, and L. Seoane, Application of the regional water mass variations from GRACE satellite gravimetry to large-scale water management in Africa, *Remote sensing*, *6*, 2014.

Rebischung, P., J. Griffiths, J. Ray, R. Schmid, X. Collilieux, and B. Garayt, IGS08: the IGS realization of ITRF2008, *GPS solutions*, *16*(4), 483–494, 2012.

Ricard, J., and J. Royer, A statistical cloud scheme for use in an AGCM, in *Annales Geophysicae*, vol. 11, pp. 1095–1115, 1993.

Schär, C., and G. Jendritzky, Climate change: hot news from summer 2003, *Nature*, *432*(7017), 559–560, 2004.

Simeonov, T., K. Vassileva, and G. Guerova, Application of ground-based GNSS meteorology in Bulgaria/Southeast Europe: case study 2007 heat wave, *Annual of University of Sofia*, *106*, 88–100, 2013.

Smith, R., A scheme for predicting layer clouds and their water content in a general circulation model, *Quarterly Journal of the Royal Meteorological Society*, *116*(492), 435–460, 1990.

Stocker, et al., *IPCC, 2013: Climate Change 2013: The Physical Science Basis. Contribution of Working Group I to the Fifth Assessment Report of the Intergovernmental Panel on Climate Change*, Cambridge University Press, Cambridge, United Kingdom and New York, NY, USA, 2013.

Swenson, S., and J. Wahr, Post-processing removal of correlated errors in GRACE data, *Geophys. Research Lett.*, *33*, 2006.

Trenberth, K. E., L. Smith, T.Qian, and J. Fasullo, Estimates of the global water budget and its annual cycle using observational and model data, *8*, 2006.

Zaitchik, B. F., M. Rodell, and R. H. Reichle, Assimilation of GRACE terrestrial water storage data into a land surface model: Results for the Mississippi river basin, *Journal of Hydrometeorology*, *9*, 535–548, 2008.